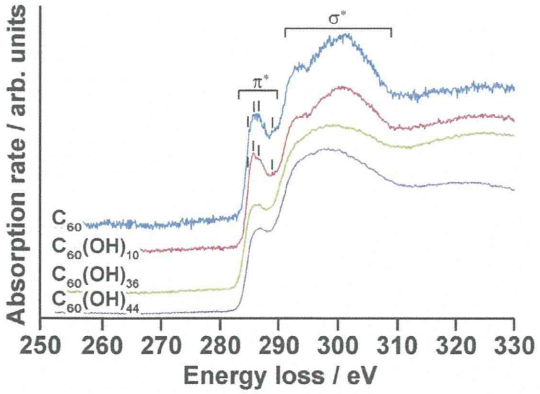

Fig. 2 – EELS in the region of the carbon *K*-shell excitation of C_{60} and its hydroxides. (A colour version of this figure can be viewed online.)

transition [28–30]. The band at around 280–287 eV includes a shoulder peak at 284.5 eV and two peaks at 285.8 and 286.3 eV. These peaks at the band and the shoulder peak at 288.3 eV are denoted by bars. The peaks at 284.5, 285.8, 286.3 and 288.3 eV are assigned to excitations into C_{60} molecular orbitals of t_{1u}, t_{1g}, (t_{2u}, h_g), and (h_u, g_g, g_u, t_g) symmetry, respectively [29,30]. Moreover, the peak at ~290 eV, which is separate from the broad band assigned to the transition to the σ^* orbital, distinguishes fullerenes from other carbon structures, such as graphite and amorphous carbon [28]. The spectrum of $C_{60}(OH)_{10}$ is very similar to that of C_{60}. However, the peak at 292 eV becomes a shoulder, which can be attributed to the hydroxylation of the C_{60} cage. The $C_{60}(OH)_{36}$ and $C_{60}(OH)_{44}$ spectra are markedly different from that of C_{60}, but resemble to that of amorphous carbon [31], which may arise from sp^2-sp^3 carbon mixture in the C_{60} cage caused by hydroxylation. The peak at 288.3 eV disappears and peaks at around 280–287 eV change to a broad band. These spectral changes and the decrease in intensity of the band relative to that of the broad band at ~300 eV indicate a distortion of symmetry and a decrease in the sp^2 character of the C_{60} cage brought by the introduction of hydroxyl groups. The peak maximum of the broad band at 300 eV is also red-shifted to 297 eV from the same reason.

We also performed EELS for $C_{60}H_{36}$ (data not shown). Although the color of the $C_{60}H_{36}$ powder indicates substantial decreases in the π-conjugation, the spectrum closely resembles that of C_{60}. The inconsistent results may be caused by the dissociation of C–H bonds of $C_{60}H_{36}$ by electron beam irradiation during the acquisition of the EELS. The results suggests that the EELS of C_{60} hydroxides are also affected by electron beam irradiation; some covalent bonds between the hydroxyl groups and the C_{60} cage of the C_{60} hydroxides are probably dissociated by electron beam irradiation. However, we propose that the marked differences in the C_{60} and $C_{60}(OH)_{10}$ spectra compared with the $C_{60}(OH)_{36}$ and $C_{60}(OH)_{44}$ spectra suggest a difference in sp^2 character.

Fig. 3a and b respectively show typical TEM images of CNHs after C_{60} was inserted from a toluene solution and after $C_{60}(OH)_{10}$ was inserted from a THF dispersion. The TEM

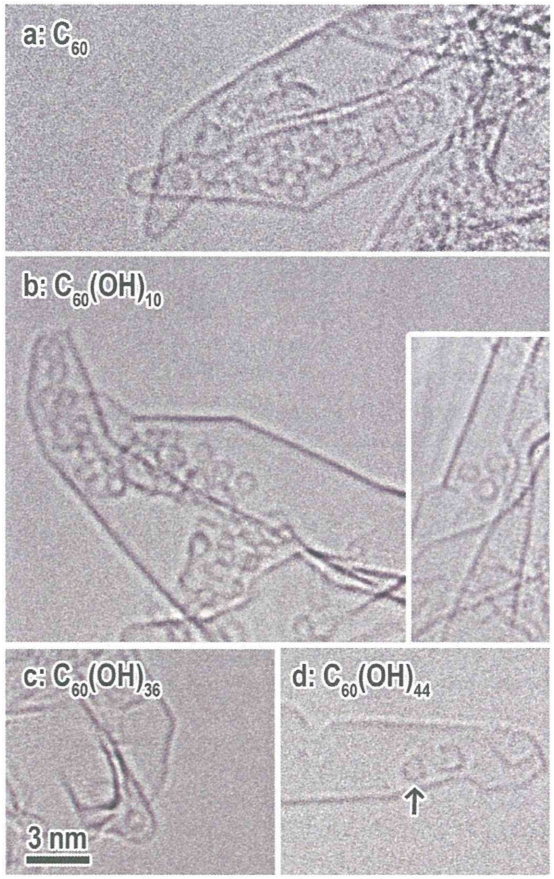

Fig. 3 – TEM images of molecules encapsulated in CNHs. (a) C_{60}, (b) $C_{60}(OH)_{10}$, (c) $C_{60}(OH)_{36}$, and (d) $C_{60}(OH)_{44}$. Note that only the structure denoted by an arrow head is a $C_{60}(OH)_{44}$ molecule and the other structures in the CNH in (d) may be parts of a decomposed molecule or contamination.

images show the efficient encapsulation of these molecules in CNHs. Furthermore, it is interesting that $C_{60}(OH)_{10}$ are encapsulated in the CNHs not from solution but from the dispersions.

Fig. 3c and d respectively show typical TEM images of CNHs after $C_{60}(OH)_{36}$ was inserted from a THF dispersion and after $C_{60}(OH)_{44}$ was inserted from a DMSO solution. These molecules maintain their spherical shell structure, even though they contain many hydroxyl groups (also see Fig. S3 in Supplementary data).

The TEM images suggest that the amount of C_{60} and the hydroxide encapsulated in the CNHs are different. For the quantitative discussion of the encapsulation of these molecules, the number of molecules encapsulated in CNHs per unit projected area in the TEM image was determined. Fig. 4 shows histograms of the number of the molecules found inside CNHs for different solvents. Error bars indicate standard deviation. The histograms show that the molecular dependences of the encapsulation from toluene, THF, and DMSO are very similar. The number of C_{60} and $C_{60}(OH)_{10}$ molecules encapsulated in the CNHs is about ten-fold the number of

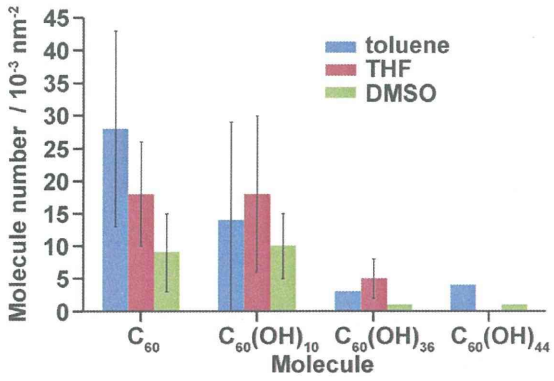

Fig. 4 – Histograms of the number of molecules as a function of molecular species per the solvents using in the preparation. Error bars in the plots indicate standard deviation.

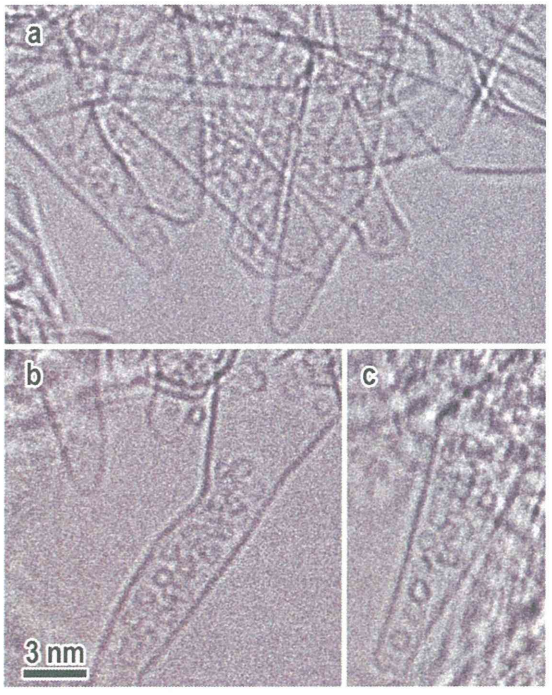

Fig. 5 – Typical TEM images of CNHs after $C_{60}H_{36}$ was inserted from a THF dispersion. The TEM images clearly show that even molecules with little sp^2 character can be encapsulated into CNHs efficiently as with cases of C_{60} and $C_{60}(OH)_{10}$.

$C_{60}(OH)_{36}$ and $C_{60}(OH)_{44}$ molecules. The number of C_{60} molecules encapsulated in the CNHs decreases as its solubility in the solvent used decreases, whereas the number of $C_{60}(OH)_{10}$ molecules is almost independent of the solvent.

Photograph of the powders (Fig. 1a) and EELS (Fig. 2) show that the sp^2 character decreases as the number of hydroxyl groups increases, and the tendency in encapsulation (Fig. 4) suggests that the sp^2 character of the C_{60} derivatives controls the encapsulation. However, this is not consistent with the large amount of $C_{60}H_{36}$ encapsulated in CNHs from toluene and THF dispersions (Fig. 5). Namely, even molecules with little sp^2 character are readily encapsulated in CNHs. Therefore, the sp^2 character is not necessarily the main factor in controlling the encapsulation. Moreover, because the molecular size of $C_{60}(OH)_{10}$ is almost the same as that of $C_{60}(OH)_{36}$ and $C_{60}(OH)_{44}$ [17–20], the molecular size is not the main factor influencing the encapsulation of C_{60} hydroxides.

Based on these discussions, we consider that the polarity of the functional groups of the C_{60} derivatives dominantly influence the encapsulation efficiency.

During the encapsulation of C_{60} by the nano-condensation method, the vaporization of the solvents results in the oversaturation of C_{60}, and C_{60} condenses on the CNH surface. The C_{60} molecules migrate on the surface pass through holes into the inner space [4]. In contrast, when C_{60} is dispersed in solvents that do not interact strongly with C_{60}, such as THF and DMSO, the C_{60} tends to form aggregates which are not encapsulated. Probably, the small amount of C_{60} dissolved in THF and DMSO are encapsulated in CNHs (Fig. 4b and c). The encapsulation of $C_{60}H_{36}$ dispersed in toluene and THF may also occur through a similar process.

In contrast, $C_{60}(OH)_{36}$ and $C_{60}(OH)_{44}$ are functionalized with many hydroxyl groups, and thus self-aggregate when the solvents are volatilized. Britz and co-workers [6] have reported similar behaviour in $C_{61}(COOH)_2$; the molecules tend to form supramolecular aggregates through hydrogen bonds between their carboxyl groups. The self-aggregation of $C_{60}(OH)_{36}$ and $C_{60}(OH)_{44}$ prevents them from entering the CNHs. The number of hydroxyl groups in $C_{60}(OH)_{10}$ may not be sufficient to cause the self-aggregation, meaning they are more efficiently incorporated in CNHs. These considerations are summarized in Fig. 6: the higher the tendency of self-aggregation caused by the increase in the number of hydroxyl groups, the lower the encapsulation efficiency.

In summary, the decrease in the sp^2 character of the C_{60} cage caused by functionalization does not influence their encapsulation efficiency. The size of the C_{60} derivative is also

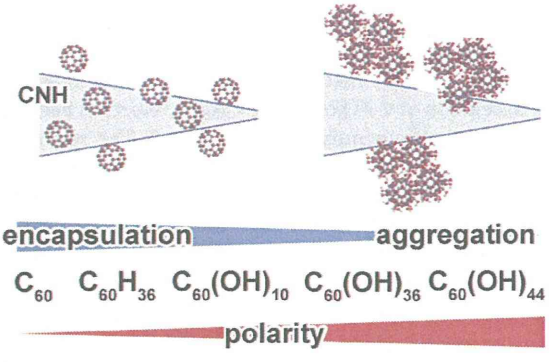

Fig. 6 – Schematic representation of the interaction between the molecules and CNHs during solvent vaporization. (A colour version of this figure can be viewed online.)

not a major factor for the encapsulation. The encapsulation difficulty of the C_{60} hydroxide molecules is due to their self-aggregation, which is determined by the interaction of the polar functional groups. The self-aggregation makes their encapsulation in CNHs difficult. Our results will allow better strategies for encapsulating various guest materials in CNHs and other nanocarbon.

An important implication of this study is that even though the sp^2 character of the C_{60} cage is decreased by functionalization, C_{60} derivatives can be encapsulated in CNHs. Moreover, it should be emphasized that the molecules can be encapsulated even from dispersion. They imply that the structure of various molecules can be studied by TEM by covalently tagging the molecules with C_{60}.

4. Conclusion

TEM observations reveal that C_{60}, $C_{60}(OH)_{10}$, and $C_{60}H_{36}$ are efficiently encapsulated in the inner space of CNHs by the nano-condensation method, using toluene, THF, and DMSO as solvents. In contrast, $C_{60}(OH)_{36}$ and $C_{60}(OH)_{44}$ are hardly encapsulated. This suggests that the polarity of functional group of the C_{60} derivatives is the main influence on the encapsulation. The sp^2 character of molecules and molecular size are not necessarily the main factor in controlling the encapsulation. Because $C_{60}(OH)_{36}$ and $C_{60}(OH)_{44}$ are very polar, they are more stabilized by self-aggregate than by dispersing on the walls of the CNHs, resulting in poor accumulation inside the CNHs.

Acknowledgment

This work was supported by KAKENHI (#25790003) from JSPS to K. Kobayashi and Health Labor Sciences Research Grants from MHLW, Japan, to K. Kokubo. The authors thank Dr. I. Hisaki (Osaka University) for guidance in the DLS measurement.

Appendix A. Supplementary data

Supplementary data associated with this article can be found, in the online version, at http://dx.doi.org/10.1016/j.carbon.2013.11.011.

REFERENCES

[1] Smith BW, Monthioux M, Luzzi DE. Encapsulated C_{60} in carbon nanotubes. Nature 1998;396(6709):323–4.
[2] Smith BW, Monthioux M, Luzzi DE. Carbon nanotube encapsulated fullerenes: a unique class of hybrid materials. Chem Phys Lett 1999;315(1–2):31–6.
[3] Smith BW, Luzzi DE. Formation mechanism of fullerene peapods and coaxial tubes: a path to large scale synthesis. Chem Phys Lett 2000;321(1–2):169–74.
[4] Yudasaka M, Ajima K, Suenaga K, Ichihashi T, Hashimoto A, Iijima S. Nano-extraction and nano-condensation for C_{60} incorporation into single-wall carbon nanotubes in liquid phases. Chem Phys Lett 2003;380(1–2):42–6.
[5] Ajima K, Yudasaka M, Suenaga K, Kasuya D, Azami T, Iijima S. Material storage mechanism in porous nanocarbon. Adv Mater 2004;16(5):397–401.
[6] Britz DA, Khlobystov AN, Wang J, O'Neil AS, Poliakoff M, Ardavanc A, et al. Selective host–guest interaction of single-walled carbon nanotubes with functionalised fullerenes. Chem Commun 2004:176–7.
[7] Liu Z, Koshino M, Suenaga K, Mrzel A, Kataura H, Iijima S. Transmission electron microscopy imaging of individual functional groups of fullerene derivatives. Phys Rev Lett 2006;96(8):088304-1-4.
[8] Liu Z, Yanagi K, Suenaga K, Kataura H, Iijima S. Imaging the dynamic behaviour of individual retinal chromophores confined inside carbon nanotubes. Nature Nanotechnol 2007;2(7):422–5.
[9] Solin N, Koshino M, Tanaka T, Takenaga S, Kataura H, Isobe H, et al. Imaging of aromatic amide molecules in motion. Chem Lett 2007;36(10):1208–9.
[10] Chamberlain TW, Camenisch A, Champness NR, Briggs GAD, Benjamin SC, Ardavan A, et al. Toward controlled spacing in one-dimensional molecular chains: alkyl-chain-functionalized fullerenes in carbon nanotubes. J Am Chem Soc 2007;129(27):8609–14.
[11] Chamberlain TW, Pfeiffer R, Peterlik H, Kuzmany H, Zerbetto F, Melle-Franco M, et al. Polyarene-functionalized fullerenes in carbon nanotubes: towards controlled geometry of molecular chains. Small 2008;4(12):2262–70.
[12] Simon F, Kuzmany H, Rauf H, Pichler T, Bernardi J, Peterlik H, et al. Low temperature fullerene encapsulation in single wall carbon nanotubes: synthesis of N@C60@SWCNT. Chem Phys Lett 2004;383(3–4):362–7.
[13] Simon F, Kuzmany H, Bernardi J, Hauke F, Hirsch A. Encapsulating C59N azafullerene derivatives inside single-wall carbon nanotubes. Carbon 2006;44(10):1958–62.
[14] Simon F, Kuzmany H, Náfrádi B, Fehér T, Forró L, Fülöp F, et al. Magnetic fullerenes inside single-wall carbon nanotubes. Phys Rev Lett 2006;97(13):136801-1-4.
[15] Okada S, Saito S, Oshiyama A. Energetics and electronic structures of encapsulated C_{60} in a carbon nanotube. Phys Rev Lett 2001;86(17):3835–8.
[16] Iwamoto T, Watanabe Y, Sadahiro T, Haino T, Yamago S. Size-selective encapsulation of C_{60} by [10]cycloparaphenylene: formation of the shortest fullerene-peapod. Angew Chem Int Ed 2011;50(36):8342–4.
[17] Kokubo K, Matsubayashi K, Tategaki H, Takada H, Oshima T. Facile synthesis of highly water-soluble fullerenes more than half-covered by hydroxyl groups. ACS Nano 2008;2(2):327–33.
[18] Kokubo K, Shirakawa S, Kobayashi N, Aoshima H, Oshima T. Facile and scalable synthesis of a highly hydroxylated water-soluble fullerenol as a single nanoparticle. Nano Res 2011;4(2):204–15.
[19] Ueno H, Kokubo K, Kwon E, Nakamura Y, Ikuma N, Oshima T. Synthesis of a new class of fullerene derivative $Li^+@C60O^-(OH)_7$ as a "cation-encapsulated anion nanoparticle". Nanoscale 2013;5(6):2317–21.
[20] Nakamura Y, Ueno H, Kokubo K, Ikuma N, Oshima T. Magic number effect on cluster formation of polyhydroxylated fullerenes in water–alcohol binary solution. J Nanopart Res 2013;15(6):1755-1-7.
[21] Iijima S, Yudasaka M, Yamada R, Bandow S, Suenaga K, Kokai F, et al. Nano-aggregates of single-walled graphitic carbon nano-horns. Chem Phys Lett 1999;309(3–4):165–70.
[22] Azami T, Kasuya D, Yuge R, Yudasaka M, Iijima S, Yoshitake T, et al. Large-scale production of single-wall carbon nanohorns with high purity. J Phys Chem C 2008;112(5):1330–4.
[23] Krätschmer W, Lamb LD, Fostiropoulos K, Huffman DR. Solid C_{60}: a new form of carbon. Nature 1990;347(6291):354–8.

[24] Rao AM, Zhou P, Wang KA, Hager GT, Holden JM, Wang Y, et al. Photoinduced polymerization of solid C_{60} films. Science 1993;259(5097):955–7.
[25] Chiang LY, Upasani RB, Swirczewski JW, Soled S. Evidence of hemiketals incorporated in the structure of fullerols derived from aqueous acid chemistry. J Am Chem Soc 1993;115(13):5453–7.
[26] She YM, Tu YP, Liu SY. C_{118} from fullerenols: formation, structure and intermolecular nC_2 transfer reactions in mass spectrometry. Rapid Commun Mass Spectrom 1996;10(6):676–8.
[27] Popov AA, Senyavin VV, Granovsky AA, Lobach AS. Vibrational spectra and molecular structure of the hydrofullerenes $C_{60}H_{18}$, $C_{60}D_{18}$, and $C_{60}H_{36}$ as studied by IR and Raman spectroscopy and first-principle calculations. In: Veziroglu TN, Zaginaichenko SYu, Schur DV, Baranowski B, Shpak AP, Skorokhod VV, editors. Hydrogen materials science and chemistry of carbon nanomaterials. Dordrecht: Kluwer Academic Publishers; 2004. p. 347–56.
[28] Saito Y, Suzuki N, Shinohara H, Hayashi T, Tomita M. Transmission electron microscopy and electron energy loss spectroscopy of C_{60} fullerite. Ultramicroscopy 1992;41(1–3):1–9.
[29] Liu X, Pichler T, Knupfer M, Golden MS, Fink J, Kataura H, et al. Filling factors, structural, and electronic properties of C_{60} molecules in single-wall carbon nanotubes. Phys Rev B 2002;65(4):045419-1-6.
[30] Sohmen E, Fink J, Krätschmer W. Electron energy-loss spectroscopy studies on C_{60} and C_{70} fullerite. Z Phys B 1992;86(1):87–92.
[31] Waidmann S, Knupfer M, Fink J, Kleinsorge B, Robertson J. Electronic structure studies of undoped and nitrogen-doped tetrahedral amorphous carbon using high-resolution electron energy-loss spectroscopy. J Appl Phys 2001;89(7):3783–92.

International Immunopharmacology 20 (2014) 258–263

Contents lists available at ScienceDirect

International Immunopharmacology

journal homepage: www.elsevier.com/locate/intimp

Effect of chemical modification on the ability of pyrrolidinium fullerene to induce apoptosis of cells transformed by JAK2 V617F mutant

Megumi Funakoshi-Tago [a,*], Masaki Tsukada [a], Toshiro Watanabe [a], Yuka Mameda [a], Kenji Tago [b], Tomoyuki Ohe [c], Shigeo Nakamura [d], Tadahiko Mashino [c], Tadashi Kasahara [a]

[a] Department of Biochemistry, Faculty of Pharmacy, Keio University, 1-5-30 Shibakoen, Minato-ku, Tokyo 105-8512, Japan
[b] Division of Structural Biochemistry, Department of Biochemistry, Jichi Medical University, 3311-1 Yakushiji, Shimotsuke-shi, Tochigi-ken 329-0498, Japan
[c] Department of Medicinal Chemistry and Bio-organic Chemistry, Faculty of Pharmacy, Keio University, 1-5-30 Shibakoen, Minato-ku, Tokyo 105-8512, Japan
[d] Department of Chemistry, Nippon Medical School, 2-297-2 Kosugi-cho, Nakahara-ku, Kawasaki, Kanagawa 211-0063, Japan

ARTICLE INFO

Article history:
Received 7 October 2013
Received in revised form 26 February 2014
Accepted 26 February 2014
Available online 12 March 2014

Keywords:
JAK2
V617F mutation
Myeloproliferative neoplasms
Pyrrolidinium fullerene
ASK1
JNK

ABSTRACT

JAK2 V617F mutant, a gene responsible for human myeloproliferative neoplasms (MPNs), causes not only cellular transformation but also resistance to various anti-cancer drugs. We previously reported that pyrrolidinium fullerene markedly induced the apoptosis of JAK2 V617F mutant-induced transformed cells through the reduction of apoptosis signal-regulating kinase 1 (ASK1), following inhibition of the c-Jun N-terminal kinase (JNK) pathway. In the current study, we found that the replacement of the 2-hydrogen atom (−H) or N-methyl group (−CH_3) by the butyl group (−C_4C_9) caused the more than 3-fold potent cytotoxic effects on cells transformed by the JAK2 V617F mutant. Strikingly, these chemical modification of pyrrolidinium fullerene resulted in more marked reduction of ASK1 protein and a more potent inhibitory effect on the JNK signaling cascade. On the other hand, when modified with a longer alkyl group, the derivatives lacked their cytotoxicity. These observations clearly indicate that the modification of pyrrolidinium fullerene with a suitable length of alkyl group such as butyl group enhances its apoptotic effect through inhibition of the ASK1-MKK4/7-JNK pathway.

1. Introduction

The myeloproliferative neoplasms (MPNs), which include polycythemia vera (PV), essential thrombocytosis (ET) and primary myelofibrosis (PMF), are clonal hematopoietic stem cell diseases characterized by uncontrolled proliferation of terminally differentiated myeloid cells. A somatic mutation of the tyrosine kinase Janus kinase 2 (JAK2) gene was identified in more than 90% of PV patients and in approximately 50% of ET and PMF patients. In the majority of MPN patients, the JAK2 gene has a homozygous G → T transversion, which results in a valine-to-phenylalanine substitution at codon 617 of JAK2 (V617F) [1–3].

Previously, we found that the JAK2 V617F mutant induces the cytokine-independent survival of erythroid progenitor cells [4]. The JAK2 V617F mutant was reported to induce the activation of signaling pathways, signal transduction and activator of transcription 3 (STAT3) and STAT5 and kinases, Akt, extracellular signal-regulated kinase (ERK) and c-Jun N-terminal kinase (JNK) in a cytokine-independent manner. We demonstrated that STAT5, Akt and JNK are critical signal transducers for the proliferation and the transforming ability induced by JAK2 V617F mutant [5–7]. In addition, it was shown that cells transformed by the JAK2 V617F mutant exhibited resistance to various anti-cancer drugs, such as bleomycin (BLM), which generates DNA double-strand breaks, and mitomycin C (MMC) and cisplatin (CDDP), which are DNA cross-linking drugs [8–11], suggesting that the JAK2 V617F mutant causes not only the activation of survival signals against apoptosis induced by cytokine removal but also the resistance to various anti-cancer drugs. Therefore, the rapid development of effective therapeutic drugs for MPNs is required.

Fullerene (C_{60}) was discovered by Kroto et al. in 1985 as the third allotropic form of carbon after diamond and graphite [12]. Fullerene is a spherical molecule 0.7 μm in diameter and a new type of organic compound with a cage-like structure [13]. Chemical modification with several hydrophilic groups increases the solubility of fullerene, and the derivatives of water-soluble fullerene were reported to possess various biological and pharmacological properties [14–18]. As a typical derivative, pyrrolidinium fullerene exhibits anti-proliferative activity to various cancer cells [19]. Previously, we reported that pyrrolidinium fullerene markedly induced apoptotic cell death of cells transformed by the JAK2 V617F mutant through reduction of the protein expression of apoptosis

Abbreviations: ASK1, apoptosis signal-regulating kinase 1; c-IAP1, cellular inhibitor of apoptosis protein 1; DCFH, dichlorodihydrofluorescein; DMSO, dimethyl sulfoxide; Epo, erythropoietin; ERK, extracellular signal-regulated kinase; EpoR, erythropoietin receptor; ET, essential thrombocytosis; JAK2, Janus kinase 2; JNK, c-Jun N-terminal kinase; MKK4/7, mitogen-activated protein kinase kinase 4/7; MPNs, myeloproliferative neoplasms; PMF, primary myelofibrosis; PV, polycythemia vera; STAT, signal transducers and activators of transcription; ROS, reactive oxygen species.

* Corresponding author. Tel./fax: +81 3 5400 2697.
E-mail address: tago-mg@pha.keio.ac.jp (M. Funakoshi-Tago).

http://dx.doi.org/10.1016/j.intimp.2014.02.035
1567-5769/

signal-regulating kinase 1 (ASK1) and inhibition of the JNK pathway [20]. ASK1, one of the mitogen-activated protein kinase kinase kinases (MAPKKKs), was previously demonstrated to stimulate the JNK signaling cascade mediating the activation of JNK upstream kinases, named MKK4/7 [21].

In the current study, we focused on the relationship between the chemical structure of the derivatives of pyrrolidinium fullerene and their apoptotic effects. Our study suggests the possibility that the chemical modification of fullerene would emphasize their utility as anti-cancer drugs.

2. Materials and methods

2.1. Chemicals and reagents

Pyrrolidinium fullerene and its derivatives were synthesized as previously described [15,17,19]. Anti β-actin antibody and anti-HA antibody (3F10) were purchased from Santa Cruz Biotechnology (Santa Cruz, CA) and Roche (Indianapolis, IN), respectively. Anti-phospho JAK2 antibody (Y1007/Y1008), anti-phospho-STAT3 antibody (Y705), anti-STAT3 antibody, anti-phospho-STAT5 antibody (Y694), anti-STAT5 antibody, anti-phospho-ERK1/2 antibody (T202/Y204), anti-ERK1/2 antibody, anti-phospho-Akt (S473), anti-Akt antibody, anti-ASK1 antibody, anti-phospho-MKK4 antibody (S257/T261), anti-MKK4 antibody, anti-phospho-MKK7 antibody (S271/T275), anti-MKK7 antibody, anti-phospho-JNK antibody (T183/Y185), anti-JNK antibody and anti-cleaved caspase 3 antibody were purchased from Cell Signaling Technology (Danvers, MA, USA). Peroxidase-conjugated secondary antibodies were from Dako (Glostrup, Denmark). 2′, 7′-dichlorofluorescin diacetate (DCFH-DA) and α-tocopherol were purchased from Sigma Inc. (St. Louis, MO).

2.2. Retroviral infection and cell cultures

Ba/F3 cells were infected with retroviruses coding a mutant of murine JAK2 c-HA (V617F) with murine EpoR as described previously [4]. The cells were cultured in RPMI 1640 medium supplemented with 10% fetal bovine serum (BioWest, Nuaillé, France), 100 units/ml penicillin (Nacalai Tesque, Tokyo, Japan) and 100 μg/ml streptomycin (Nacalai Tesque).

2.3. Western blotting

Cells were harvested in ice-cold PBS and lysed in Nonidet P-40 lysis buffer (50 mM Tris-HCl, pH 8.0, 120 mM NaCl, 1 mM EDTA pH 8.0, 0.5%

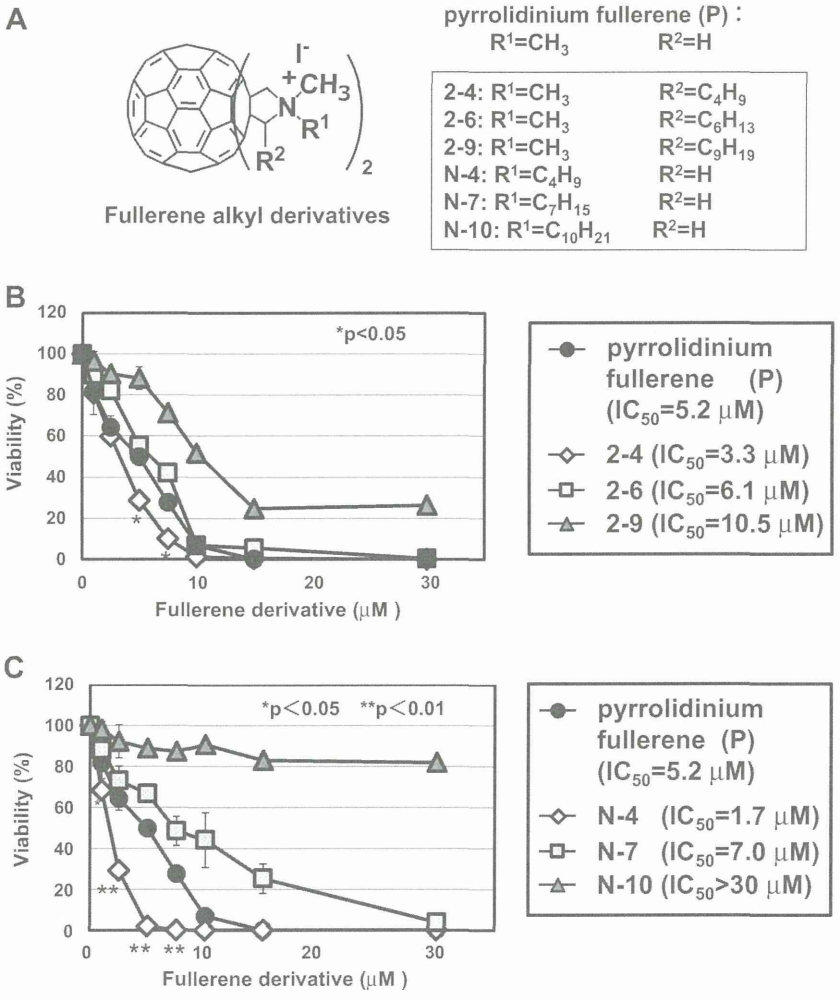

Fig. 1. Pyrrolidinium fullerene and its derivatives exhibit cytotoxicity to VF-Ba/F3 cells. (A) Structures of fullerene derivatives. Pyrrolidinium fullerene (P) is C_{60}-bis *N*, *N*-dimethylpyrrolidinium iodide. In pyrrolidinium fullerene (P), the 2-hydrogen atom (−H) or N-methyl group ($-CH_3$) was substituted with various alkyl groups and named 2-4, 2-6, 2-9, N-4, N-7, and N-10, respectively. (B, C) VF-Ba/F3 cells were treated with different concentrations (1, 2.5, 5, 7.5, 10, 15, 30 μM) of pyrrolidinium fullerene (P) and its derivatives for 24 h. Cell viability was determined by trypan blue staining. Results are the mean ± S.D. of three independent experiments. * and ** indicate significant differences at $p < 0.05$ and $p < 0.01$, respectively (vs pyrrolidinium fullerene (P)).

Nonidet P-40, 10 mM β-glycerophosphate, 2.5 mM NaF, 0.1 mM Na_3VO_4) supplemented with protease inhibitors. Denatured samples were resolved by SDS-PAGE and transferred to polyvinylidene difluoride membranes (Millipore, Billerica, MA). Membranes were probed using the designated antibodies and visualized with the ECL detection system (GE Healthcare, Little Chalfont, United Kingdom) [4].

2.4. Measurement of cell viability and cell cycle analysis

Transduced Ba/F3 cells were incubated with RPMI 1640 medium supplemented with 1% fetal bovine serum. Cells were treated with DMSO (0.1%) or various concentrations of pyrrolidinium fullerene derivatives for 24 h. Cell viability was checked by the trypan blue exclusion method. Cell cycle parameters were determined by flow-cytometry analysis using FACSCalibur (BD Biosciences, San Jose, CA) [5].

2.5. DNA fragmentation assay

Genomic DNA was prepared for gel electrophoresis as described previously [5]. Electrophoresis was performed on a 1% agarose gel in Tris/boric acid/EDTA buffer.

2.6. Measurement of ROS generation

Cells were incubated with DCFH-DA (2′, 7′-dichlorodihydrofluorescein-DA), a permeable fluorescence probes (10 μM) for 15 min and washed with PBS. Then, cells were treated with each fullerene derivative at indicated concentration for 1 h, and the fluorescence intensity of oxidized DCF was monitored using FACSCalibur with the CELL Quest program as previously described [19]. To test the effect of α-tocopherol, cells were pre-treated with α-tocopherol (300 μM) for 1 h prior to the treatment with fullerene derivative.

2.7. Data presentation

All of the experiments were independently performed at least 3 times. Error bar means standard deviation (S.D.).

3. Results

3.1. Effects of pyrrolidinium fullerene derivatives on the viability of VF-Ba/F3 cells

A previous study showed that pyrrolidinium fullerene induced apoptotic cell death of Ba/F3 cells transformed by the JAK2 V617F mutant (VF-Ba/F3 cells) [20]. To test the effect of chemical modification on the cytotoxicity of pyrrolidinium fullerene, 6 types of derivatives were newly synthesized from pyrrolidinium fullerene as the lead compound. As shown in Fig. 1A, derivatives named 2-4, 2-6 and 2-9 are compounds in which the 2-hydrogen atom (−H) in pyrrolidinium fullerene was replaced by a butyl group ($-C_4H_9$), hexyl group ($-C_6H_{13}$) and nonyl group ($-C_9H_{19}$), respectively. In three other derivatives, named N-4, N-7 and N-10, the N-methyl group ($-CH_3$) in pyrrolidinium fullerene was replaced by a butyl group ($-C_4H_9$), heptyl group ($-C_7H_{15}$) and decyl group ($-C_{10}H_{21}$), respectively. First, we tested the effects of these two groups of derivatives on the viability of VF-Ba/F3 cells. Compared to original pyrrolidinium fullerene, 2-4 more effectively induced the cell death of VF-Ba/F3 cells, while the cytotoxicity of 2-6 and 2-9 was comparable and lower than the original compound, respectively. In the next derivative's group, only N-4 showed more effective cytotoxicity. The cytotoxicity of N-7 was lower than the original compound and N-10 had no effect on the viability of VF-Ba/F3 cells (Fig. 1C). JAK2 V617F mutant-transformed cells exhibited higher sensitivity against these two derivatives, 2-4 and N-4, than the original pyrrolidinium fullerene. IC_{50} of derivatives 2-4 and N-4 was 3.3 μM and 1.7 μM, respectively, while IC_{50} of pyrrolidinium fullerene was 5.2 μM.

3.2. Apoptosis induction of VF-Ba/F3 cells by pyrrolidinium fullerene derivatives

In the previous study, pyrrolidinium fullerene exhibited apoptotic effects on VF-Ba/F3 cells. Therefore, we tested whether the derivatives could induce apoptotic cell death of VF-Ba/F3 cells. As in the previous study, the original pyrrolidinium fullerene resulted in the accumulation of sub-G1 phase, an index to evaluate apoptosis in a dose-dependent

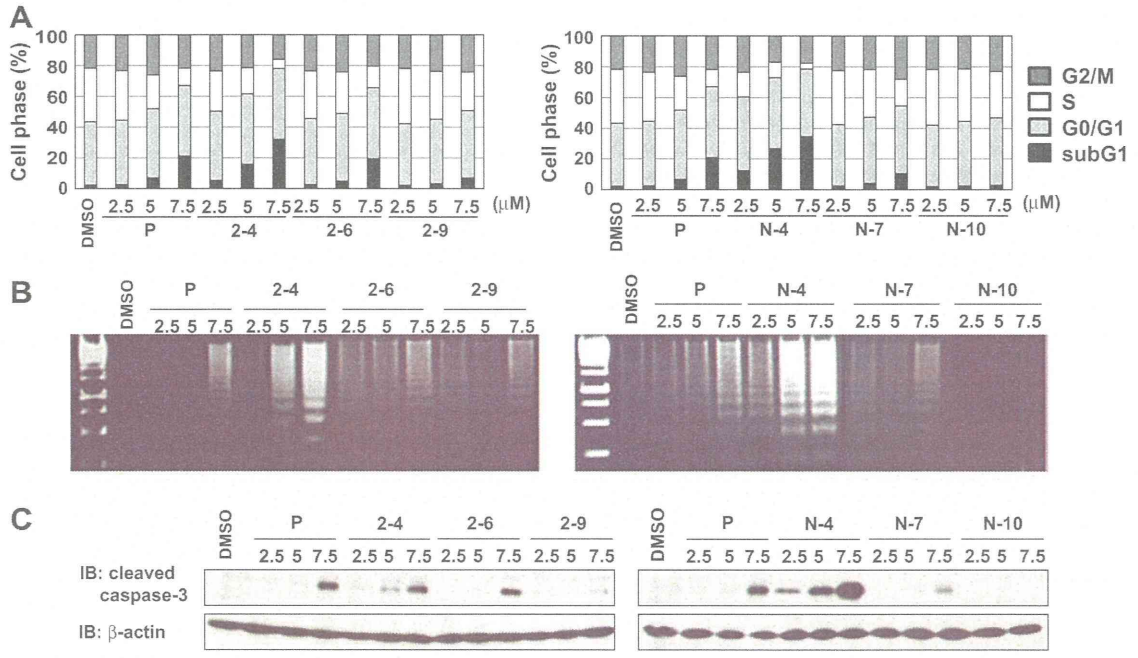

Fig. 2. Pyrrolidinium fullerene and its derivatives induce apoptosis of VF-Ba/F3 cells. VF-Ba/F3 cells were treated with DMSO (0.1%), pyrrolidinium fullerene (P) or its derivatives, 2-4, 2-6, 2-9, N-4, N-7, and N-10 (2.5, 5, 7.5 μM), for 24 h. (A) Cells were fixed, treated with propidium iodide and subjected to flow-cytometry analysis. (B) DNA was isolated from cells and subjected to agarose gel electrophoresis. (C) Cell lysates were prepared and immunoblotted with anti-cleaved caspase-3 antibody or anti-β-actin antibody.

manner (Fig. 2). In the first derivative's group, only 2-4 showed higher efficiency to induce Sub-G1 accumulation, while the others, 2-6 and 2-9, were comparable and weaker, respectively. Similarly, in the next derivative's group, only N-4 showed a higher apoptotic effect against VF-Ba/F3 cells. It is also notable that 2-4 and N-4 showed apoptotic effects at a lower concentration (5 μM), and these observations well fitted the observed results in Fig. 1. The ladder pattern of DNA internucleosomal fragmentation and the cleavage of caspase-3 were other suitable indexes to evaluate apoptosis. We next tested the effects of derivatives of pyrrolidinium fullerene on DNA fragmentation and caspase-3 activation. DNA fragmentation was clearly detected in VF-Ba/F3 cells treated with 2-4 and N-4 at 5 μM, while pyrrolidinium fullerene and 2-6 showed similar effects at a higher concentration (7.5 μM) (Fig. 2B). Notably, derivatives 2-4 and N-4 showed similar effects on caspase-3 activation (Fig. 2C). These data clearly suggested that the chemical modification of pyrrolidinium fullerene with a butyl group at a suitable position enhances its cytotoxicity.

3.3. Pyrrolidinium fullerene derivatives caused apoptosis in ROS-independent manner

Next, we tested the ability of pyrrolidinium fullerene derivatives to induce ROS generation. Derivatives 2-4, 2-6 and N-4 comparably caused ROS generation like unmodified pyrrolidinium fullerene. On the other hand, derivative 2-9 exhibited slightly lower activity to induce ROS generation, and N-7 and N-10 failed to induce ROS generation in VF-Ba/F3 cells (Fig. 3A). Next, to test whether oxidative stress is involved in their cytotoxic effects against VF-Ba/F3 cells, the effect of an antioxidant, α-tocopherol was analyzed. Pretreatment with α-tocopherol significantly suppressed ROS generation induced by pyrrolidinium fullerene and its derivatives, 2-4, 2-6, 2-9 and N-4 (Fig. 3B). However, α-tocopherol failed to cancel their cytotoxic effects (Fig. 3C). These results suggest that fullerene derivatives cause apoptotic effects against VF-Ba/F3 cells through ROS-independent mechanisms.

3.4. Effects of pyrrolidinium fullerene derivatives on the expression of ASK1 protein and JNK signaling cascade in VF-Ba/F3 cells

Previously, we showed that pyrrolidinium fullerene reduced the expression level of ASK1 by the proteasome pathway, resulting in the inhibition of its downstream molecules, including MKK4, MKK7 and JNK, which are important for the survival and proliferation of VF-Ba/F3 cells [20]. Next, the effects of fullerene derivatives on the expression of ASK1 in VF-Ba/F3 cells were examined. Interestingly, derivatives 2-4 and N-4 reduced the expression of ASK1 protein more strongly than treatment with pyrrolidinium fullerene. Furthermore, derivatives 2-4 and N-4 exhibited a more potent inhibitory effect on the activation of MKK4, MKK7 and JNK than pyrrolidinium fullerene, and the inhibitory effect of N-4 was particularly high. The inhibitory effect of 2-6 on ASK1 expression and the phosphorylation of MKK4, MKK7 and JNK was equivalent to the effect of pyrrolidinium fullerene, and the inhibitory effect of 2-9 was lower than pyrrolidinium fullerene. On the other hand, derivatives N-7 and N-10 had little effect on ASK1 expression and activation of MKK4, MKK7 and JNK (Fig. 4A, B). On the other hand, these compounds failed to inhibit other signaling molecules including JAK2, STAT5, ERK and Akt (Supplemental Fig. 1S). Notably, the tendency towards the reduction of ASK1 protein and inhibitory effects on ASK1 downstream signals caused by pyrrolidinium fullerene and its derivatives are well correlated with the strength of their ability to induce apoptosis of VF-Ba/F3 cells.

4. Discussion

As reported previously, JAK2 V617F mutant-induced transformed cells show resistance to various anti-tumor drugs in comparison with untransformed cells [20]. Here, we showed that pyrrolidinium fullerene

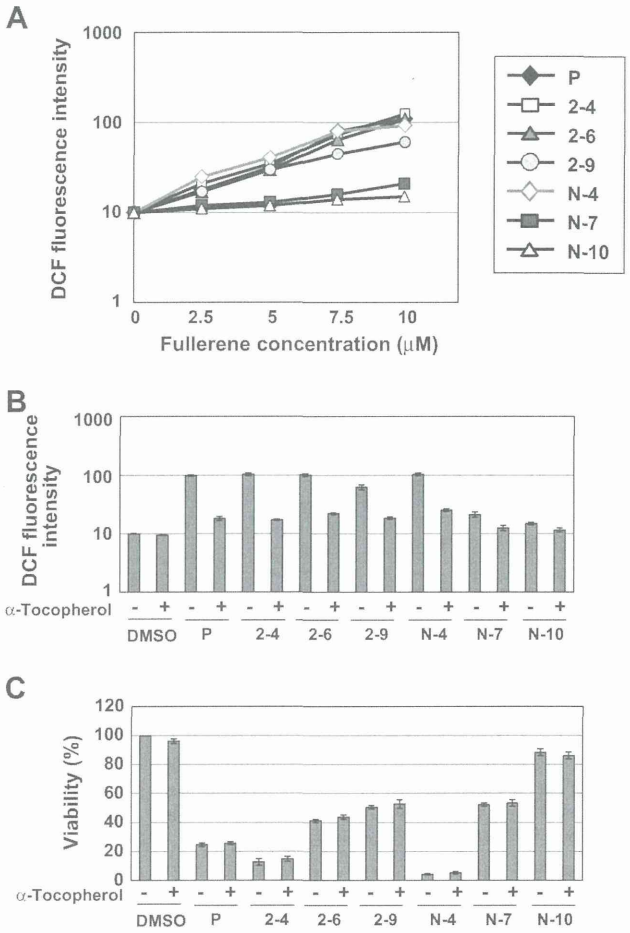

Fig. 3. Pyrrolidinium fullerene and derivatives 2-4 and N-4 induced apoptosis of VF-Ba/F3 cells independently of ROS production. (A) VF-Ba/F3 cells were incubated with DCFH-DA fluorescence probes (10 μM) for 15 min and treated with DMSO (0.1%), pyrrolidinium fullerene or its derivatives, 2-4, 2-6, 2-9, N-4, N-7, and N-10 (2.5, 5, 7.5, 10 μM), for 1 h. Oxidative stress was measured using DCFH-DA fluorescence probes. (B, C) VF-Ba/F3 cells were incubated with DCFH-DA fluorescence probes (10 μM) for 15 min and then pre-incubated with α-tocopherol (300 μM) for 1 h before exposure to DMSO (0.1%) or fullerene derivatives (7.5 μM) for 1 h. (B) Oxidative stress was measured using DCFH-DA fluorescence probes. (C) Cell viability was determined by trypan blue staining. Data are the mean ± S.D. of the relative expression levels in three experiments.

potently induced apoptosis of the cells transformed by JAK2 V617F mutant by inhibiting JNK activation. This finding suggests that pyrrolidinium fullerene can be used as a new MPN therapeutic drug. In the current study, we additionally found that the chemical modification of pyrrolidinium fullerene with a butyl group enhanced its cytotoxicity (Fig. 5).

It has been well established that fullerene derivatives show biological effects by mediating the production of ROS [19,20]. We also examined the effect of the modification of pyrrolidinium fullerene with alkyl groups of various lengths. It was found that the modification of pyrrolidinium fullerene with alkyl groups enhanced the cytotoxicity to HL-60 cells, and their effects depended on the length of the introduced alkyl groups (data not shown). Their cytotoxicity to HL-60 cells was effectively abolished by pretreatment with α-tocopherol, suggesting that their cytotoxic effects against HL-60 cells were mediated by the production of ROS. However, in the case of VF-Ba/F3 cells, pyrrolidinium fullerene modified with a butyl group caused the apoptotic effect, not through ROS production (Fig. 3). These findings clearly suggest that alkyl pyrrolidinium fullerenes cause cytotoxicity by affecting various signaling pathways, depending on the type of target cells. However,

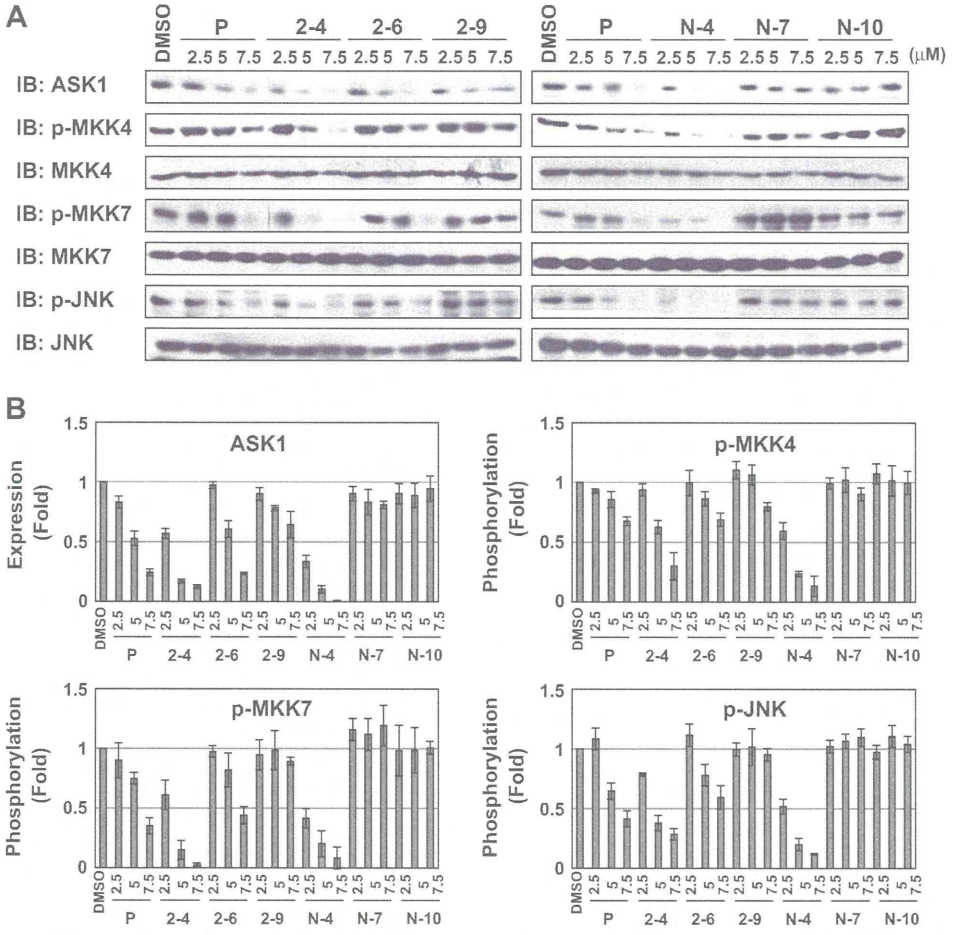

Fig. 4. Derivatives 2-4 and N-4 cause protein reduction of ASK1 and inhibit JNK signaling cascade. (A, B) VF-Ba/F3 cells were treated with DMSO (0.1%), pyrrolidinium fullerene (P), or its derivatives, 2-4, 2-6, 2-9, N-4, N-7, and N-10 (2.5, 5, 7.5 μM) for 16 h. (A) Cell lysates were immunoblotted with anti-ASK1 antibody, anti-phospho-MKK4 antibody (S257/T261), anti-MKK4 antibody, anti-phospho-MKK7 antibody (S271/T275), anti-MKK7 antibody, anti-phospho-JNK antibody (T183/Y185), anti-JNK antibody or anti-β-actin antibody. (B) The expression level of ASK1 was normalized with the expression level of β-actin. The phosphorylation levels of MKK4, MKK7 and JNK were normalized with the expression level of these molecules. The fold expression of ASK1 and the fold phosphorylation of MKK4, MKK7 and JNK are shown in graphs. Data are the mean ± S.D. of the relative expression levels in three experiments.

it is still unknown what causes the differences in the response to pyrrolidinium fullerene and its derivatives in target cells.

A number of studies have reported the importance of the JNK signaling cascade for anti-apoptotic and oncogenic signals. Previously, we observed that a specific JNK inhibitor, SP600125, significantly induced the apoptosis of VF-Ba/F3 cells. In addition, inhibition of JNK reduced the expression of c-Myc, a proto-oncogene product contributing to the transforming activity of JAK2 V617F mutant [20–24]. The JNK

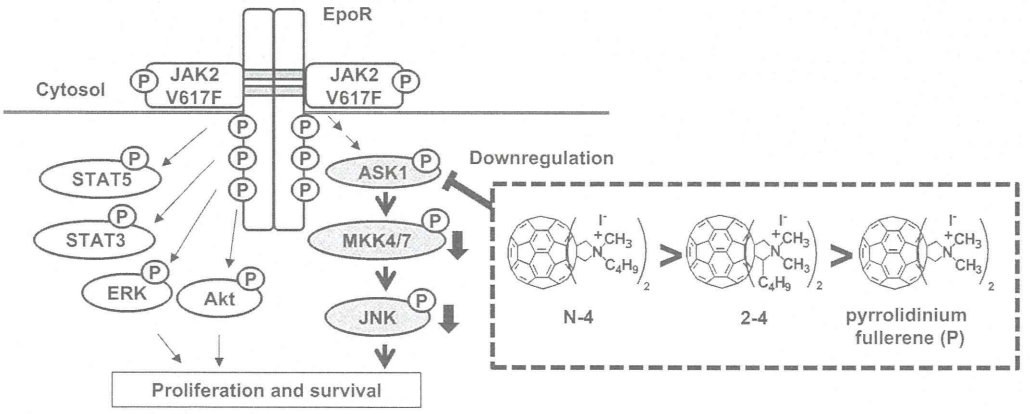

Fig. 5. Inhibitory mechanism of JAK2 V617F mutant-induced signaling pathway by pyrrolidinium fullerene derivatives. Pyrrolidinium fullerene (P) reduces the expression of ASK1, resulting in inhibition of the phosphorylation of MKK4, MKK7 and JNK, and induces apoptotic cell death of VF-Ba/F3 cells. The replacement of the 2-hydrogen atom (−H) or N-methyl group ($-CH_3$) with a butyl group ($-C_4H_9$) enhanced the ability of pyrrolidinium fullerene to induce apoptosis. In particular, replacement with a butyl group at 2-H more effectively enhanced the ability of pyrrolidinium fullerene to induce apoptosis.

signaling pathway has been reported to inactivate a pro-apoptotic protein, Bad, through its phosphorylation [25]. Although we did not test the effect of pyrrolidinium fullerene on the phosphorylation of Bad, this will be an important issue to be clarified in the near future.

Notably, we found that the cytotoxicity caused by pyrrolidinium fullerenes was well correlated with the tendency of ASK1 reduction in VF-Ba/F3 cells (Fig. 4). Previously, we showed that the down-regulation of ASK1 by pyrrolidinium fullerene was abolished by a proteasome inhibitor MG132, suggesting that pyrrolidinium fullerene caused ASK1 degradation by the proteasome pathway [20]. ROS generation activates ASK1 through the oxidation of an ASK1 inhibitor, thioredoxin [26]. Although pyrrolidinium fullerene and its derivatives induce ROS generation, this does not contribute to the activation of ASK1 and its downstream signals (Fig. 4). Yu et al. reported that JAK2 controls the expression level of ASK1 by directly phosphorylating ASK1 at tyrosine 718 [27]. However, we observed that the expression level of ASK1 was not affected by the expression of JAK2 V617F mutant, suggesting that JAK2-mediated stabilization of ASK1 seems to depend on the cell type.

The cellular inhibitor of apoptosis protein 1 (c-IAP1) was identified as the E3 ubiquitin ligase for ASK1 in the TNFα signaling pathway [28]. Although the detailed mechanism of how pyrrolidinium fullerene induces the degradation of ASK1 is unclear, pyrrolidinium fullerene and its derivatives may prompt the proteasomal degradation of ASK1 through ubiquitination by c-IAP1. Identification of the target protein of pyrrolidinium fullerenes will be a very important issue in future studies of pyrrolidinium fullerenes as anti-tumor drugs.

Supplementary data to this article can be found online at http://dx.doi.org/10.1016/j.intimp.2014.02.035.

Acknowledgments

We thank Dr. J. N. Ihle for the retroviral vectors of JAK2 and EpoR. This work was supported in part by grants (23790096, 21590072) from MEXT, Takeda Science Foundation, the Uehara Memorial Foundation and Keio Gijuku Fukuzawa Memorial Fund for the Advancement of Education and Research. This work was also supported by the Platform for Drug Discovery, Informatics, and Structural Life Science from the Ministry of Education, Culture, Sports, Science and Technology, Japan (25460073).

References

[1] James C, Ugo V, Le Couédic JP, Staerk J, Delhommeau F, Lacout C, et al. A unique clonal JAK2 mutation leading to constitutive signalling causes polycythaemia vera. Nature 2005;434(7037):1144–8.
[2] Kralovics R, Passamonti F, Buser AS, Teo SS, Tiedt R, Passweg JR, et al. A gain-of-function mutation of JAK2 in myeloproliferative disorders. N Engl J Med 2005;352(17):1779–90.
[3] Levine RL, Wadleigh M, Cools J, Ebert BL, Wernig G, Huntly BJ, et al. Activating mutation in the tyrosine kinase JAK2 in polycythemia vera, essential thrombocythemia, and myeloid metaplasia with myelofibrosis. Cancer Cell 2005;7(4):387–97.
[4] Funakoshi-Tago M, Pelletier S, Moritake H, Parganas E, Ihle JN. Jak2 FERM domain interaction with the erythropoietin receptor regulates Jak2 kinase activity. Mol Cell Biol 2008;28(5):1792–801.
[5] Abe M, Funakoshi-Tago M, Tago K, Kamishimoto J, Aizu-Yokota E, Sonoda Y, et al. The polycythemia vera-associated Jak2 V617F mutant induces tumorigenesis in nude mice. Int Immunopharmacol 2009;9(7–8):870–7.
[6] Funakoshi-Tago M, Tago K, Abe M, Sonoda Y, Kasahara T. STAT5 activation is critical for the transformation mediated by myeloproliferative disorder-associated JAK2 V617F mutant. J Biol Chem 2010;285(8):5296–307.
[7] Kamishimoto J, Tago K, Kasahara T, Funakoshi-Tago M. Akt activation through the phosphorylation of erythropoietin receptor at tyrosine 479 is required for myeloproliferative disorder-associated JAK2 V617F mutant-induced cellular transformation. Cell Signal 2011;23(5):849–56.
[8] Plo I, Nakatake M, Malivert L, de Villartay JP, Giraudier S, Villeval JL, et al. JAK2 stimulates homologous recombination and genetic instability: potential implication in the heterogeneity of myeloproliferative disorders. Blood 2008;112(4):1402–12.
[9] Sumi K, Tago K, Kasahara T, Funakoshi-Tago M. Aurora kinase A critically contributes to the resistance to anti-cancer drug cisplatin in JAK2 V617F mutant-induced transformed cells. FEBS Lett 2011;585(12):1884–90.
[10] Nakatake M, Monte-Mor B, Debili N, Casadevall N, Ribrag V, Solary E, et al. JAK2(V617F) negatively regulates p53 stabilization by enhancing MDM2 via La expression in myeloproliferative neoplasms. Oncogene 2012;31(10):1323–33.
[11] Ueda F, Sumi K, Tago K, Kasahara T, Funakoshi-Tago M. Critical role of FANCC in JAK2 V617F mutant-induced resistance to DNA cross-linking drugs. Cell Signal 2013;25(11):2115–24.
[12] Kroto H, Heath JR, O'Brien SC, Curl RF, Smalley RE. Nature 1995;318:162–3.
[13] Kroto H. Space, stars, c60, and soot. Science 1988;242(4882):1139–45.
[14] Mashino T, Shimotohno K, Ikegami N, Nishikawa D, Okuda K, Takahashi K, et al. Human immunodeficiency virus-reverse transcriptase inhibition and hepatitis C virus RNA-dependent RNA polymerase inhibition activities of fullerene derivatives. Bioorg Med Chem Lett 2005;15(4):1107–9.
[15] Nakamura S, Mashino T. Water-soluble fullerene derivatives for drug discovery. J Nippon Med Sch 2012;79(4):248–54.
[16] Mashino T, Usui N, Okuda K, Hirota T, Mochizuki M. Respiratory chain inhibition by fullerene derivatives: hydrogen peroxide production caused by fullerene derivatives and a respiratory chain system. Bioorg Med Chem 2003;11(7):1433–8.
[17] Mashino T, Nishikawa D, Takahashi K, Usui N, Yamori T, Seki M, et al. Antibacterial and antiproliferative activity of cationic fullerene derivatives. Bioorg Med Chem Lett 2003;13(24):4395–7.
[18] Shoji M, Takahashi E, Hatakeyama D, Iwai Y, Morita Y, Shirayama R, et al. Anti-influenza activity of c60 fullerene derivatives. PLoS One 2013;8(6):e66337.
[19] Nishizawa C, Hashimoto N, Yokoo S, Funakoshi-Tago M, Kasahara T, Takahashi K, et al. Pyrrolidinium-type fullerene derivative-induced apoptosis by the generation of reactive oxygen species in HL-60 cells. Free Radic Res 2009;43(12):1240–7.
[20] Funakoshi-Tago M, Nagata T, Tago K, Tsukada M, Tanaka K, Nakamura S, et al. Fullerene derivative prevents cellular transformation induced by JAK2 V617F mutant through inhibiting c-Jun N-terminal kinase pathway. Cell Signal 2012;24(11):2024–34.
[21] Ichijo H, Nishida E, Irie K, ten Dijke P, Saitoh M, Moriguchi T, et al. Induction of apoptosis by ASK1, a mammalian MAPKKK that activates SAPK/JNK and p38 signaling pathways. Science 1997;275(5296):90–4.
[22] Wang C, Mayer JA, Mazumdar A, Fertuck K, Kim H, Brown M, et al. Estrogen induces c-myc gene expression via an upstream enhancer activated by the estrogen receptor and the AP-1 transcription factor. Mol Endocrinol 2011;25(9):1527–38.
[23] Iavarone C, Catania A, Marinissen MJ, Visconti R, Acunzo M, Tarantino C, et al. The platelet-derived growth factor controls c-myc expression through a JNK- and AP-1-dependent signaling pathway. J Biol Chem 2003;278(50):50024–30.
[24] Funakoshi-Tago M, Sumi K, Kasahara T, Tago K. Critical roles of Myc-ODC axis in the cellular transformation induced by myeloproliferative neoplasm-associated JAK2 V617F mutant. PLoS One 2013;8(1):e52844.
[25] Deng H, Zhang J, Yoon T, Song D, Li D, Lin A. Phosphorylation of Bcl-associated death protein (Bad) by erythropoietin-activated c-Jun N-terminal protein kinase 1 contributes to survival of erythropoietin-dependent cells. Int J Biochem Cell Biol 2011;43(3):409–15.
[26] Liu H, Nishitoh H, Ichijo H, Kyriakis JM. Activation of apoptosis signal-regulating kinase 1 (ASK1) by tumor necrosis factor receptor-associated factor 2 requires prior dissociation of the ASK1 inhibitor thioredoxin. Mol Cell Biol 2000;20(6):2198–208.
[27] Yu L, Min W, He Y, Qin L, Zhang H, Bennett AM, et al. JAK2 and SHP2 reciprocally regulate tyrosine phosphorylation and stability of proapoptotic protein ASK1. J Biol Chem 2009;284(20):13481–8.
[28] Zhao Y, Conze DB, Hanover JA, Ashwell JD. Tumor necrosis factor receptor 2 signaling induces selective c-IAP1-dependent ASK1 ubiquitination and terminates mitogen-activated protein kinase signaling. J Biol Chem 2007;282(11):7777–82.